Polarized Fluorescence and Absorption of Macroscopically Aligned Light Harvesting Complex II

Herbert van Amerongen, Stefan L. S. Kwa, Bauke M. van Bolhuis, and Rienk van Grondelle
Department of Physics and Astronomy and Institute for Molecular Biological Sciences, Vrije Universiteit, De Boelelaan 1081, 1081 HV Amsterdam, The Netherlands

ABSTRACT Polarized absorption and fluorescence measurements have been performed at 77 K on isotropic and anisotropic preparations of trimeric Light Harvesting Complex II (LHC-II) from spinach. The results enable a decomposition of the absorption spectrum into components parallel and perpendicular to the trimeric plane. For the first time, it is shown quantitatively that the strong absorption band around 676 nm is polarized essentially parallel to the plane of the trimer, i.e., the average angle between the corresponding transition dipole moments and this plane is at most 12°. The different absorption bands for LHC-II should not be considered as corresponding to individual pigments but to collective excitations of different pigments. Nevertheless, the average angle between the Q_y transition dipole moments of all chlorophyll *a* pigments in LHC-II and the trimeric plane could be determined and was found to be 17.5° ± 2.5°. For the chlorophyll *b* pigments, this angle is significantly larger (close to 35°). At 77 K, most of the fluorescence stems from a weak band above 676 nm and the corresponding transition dipole moments are oriented further out of plane than the dipole moments corresponding to the 676-nm band. The results are shown to be of crucial significance for understanding the relation between the LHC-II structure and its spectroscopy.

INTRODUCTION

The most abundant pigment-protein complex in green plants is light-harvesting complex II (LHC-II). It binds approximately 50% of all chlorophylls (Kühlbrandt and Wang, 1991) and functions as an antenna that effectively absorbs sunlight. Induced excitations are transported mainly to the reaction center of Photosystem II where the transformation of the excitation energy into useful chemical energy is performed.

In 1991, the crystal structure of LHC-II was published at 6-Å resolution (Kühlbrandt and Wang, 1991), and significant progress has recently been achieved, resulting in the structure at 3.4-Å resolution (Kühlbrandt and Wang, 1994). The 6 Å crystal structure shows a trimeric arrangement of the protein, and in each monomeric subunit 13–15 structures could be resolved with chlorophyll-like shapes (Kühlbrandt and Wang, 1991). The 3.4-Å structure reveals that, in reality, only 12 of these correspond to chlorophyll molecules (Kühlbrandt and Wang, 1994). Recently, detailed spectroscopic information on trimeric LHC-II was obtained especially in the absorption region of the Q_y transitions of Chl *a* and Chl *b* (640–700 nm) at low temperatures (4K, 77K) (Hemelrijk et al., 1992; Kwa et al., 1992a). The complexes were isolated with the use of the detergent dodecylmaltoside, and especially the linear dichroism (LD) and circular dichroism (CD) spectra showed significant resemblance to the spectra of thylakoid membranes in which the LHC-II protein prevails. This indicates that the isolated LHC-II strongly resembles the in vivo form.

Many spectral forms are present in the antenna complex, and strong excitonic interactions between the pigments exist, as can be anticipated from the dense packing of the pigments (Kühlbrandt and Wang, 1991). The almost perfect agreement between the shape of the reduced linear dichroism spectrum and the excitation anisotropy spectrum below 676 nm indicates that fast excitation energy equilibration between the pigments in the different monomeric subunits occurs upon excitation below 676 nm (Hemelrijk et al., 1992; Kwa et al., 1992b). In different studies, energy transfer steps in LHC-II were observed on a time scale of several hundreds of femtoseconds to several picoseconds (Gillbro et al., 1985; Eads et al., 1989). Isotropic room temperature pump-probe measurements showed fast spectral equilibration on a time scale of less than 10 ps, and polarized pump-probe measurements also showed fast depolarization on a similar time scale (Kwa et al., 1992b). The wavelength dependence of the residual anisotropy at room temperature is in qualitative agreement with what one would expect from the LD spectrum in the case of fast rotational equilibration (see Theory). In recent pump-probe experiments, it was observed that even down to temperatures as low as 13 K the kinetic behavior is very similar to that at room temperature upon excitation at 676 nm and below (Savikhin et al., 1994, in press). The fluorescence lifetime of LHC-II is on the order of several nanoseconds (Ide et al., 1987), which is much longer than the rotational equilibration time. This is a necessary condition to finally trap virtually all excitations in the reaction center. For the present study, this fact is important for the interpretation of the results.

Data have been obtained concerning the qualitative orientations of absorption and emission dipole moments within LHC-II (Hemelrijk et al., 1992; Kwa et al., 1992a). To relate

Received for publication 7 December 1993 and in final form 9 May 1994.
Address reprint requests to Herbert van Amerongen, Department of Physics and Astronomy, Vrije Universiteit, De Boelelaan 1081, 1081 HV Amsterdam, The Netherlands. Tel.: 011-31-20-4447932; Fax.: 011-31-20-4447899.

Abbreviations used: LD, linear dichroism; D, circular dichroism; LHC-II, Light Harvesting Complex II, Chl *a*, chlorophyll a, Chl *b*, chlorophyll b; *A*, isotropic absorption; ΔA, amount of linear dichroism; *r*, fluorescence anisotropy.

0006-3495/94/08/837/11 $2.00

the spectroscopic properties of LHC-II to its three-dimensional structure in as much detail as possible, it is absolutely necessary to obtain more quantitative information on the orientations of the transition dipole moments. This information can be only partly obtained from linear dichroism measurements. Knowledge about the degree of orientation of the complexes in the sample is required in this respect, which has to be obtained from additional techniques.

It has been shown for chlorosomes from the green bacterium *Chloroflexus aurantiacus* and B800–850 pigment-protein complexes from the purple bacterium *Rhodobacter sphaeroides* that the degree of orientation can be obtained from polarized steady-state fluorescence measurements on complexes in compressed gels, provided that the complexes show optical rotational symmetry (see below) and fast rotational excitation equilibration takes place (Van Amerongen et al., 1991). In the present study, this method is extended and applied for the study of LHC-II to reveal the (average) orientations of the absorption and emission transition dipole moments. This leads to the decomposition of the absorption spectrum of LHC-II into components parallel and perpendicular to the C_3-symmetry axis. The presence of many absorption bands (at least 36 chlorophyll pigments are present per trimer) in a limited wavelength region (40 nm) precludes a description of the "parallel and perpendicular spectra" in terms of all its constituting bands (at least 11 bands have been revealed so far with different techniques (Reddy et al., 1994; S. Nußberger, J. P. Dekker, W. Kühlbrandt, B. M. van Bolhuis, R. van Grondelle and H. van Amerongen, unpublished data). Nevertheless, important information is obtained that is essential for future studies, aimed at the correlation between the crystal structure and the spectroscopic properties, which is required for understanding the functioning of the protein:

(1) The average orientation of the transition dipole moments that correspond to the dominant 676 nm band have been determined accurately. This information severely restricts the possible orientations of the many (at least 12) Chl *a* pigments per trimer that contribute to this band (Hemelrijk et al., 1992).

(2) The average orientations of the Q_y transition dipole moments of both the individual Chl *a* pigments and the individual Chl *b* pigments are obtained. These turn out to be significantly different. This information will restrict the possible assignments of the identities of the chlorophyll molecules (either Chl *a* or Chl *b*). Note that the identity of these pigments cannot be revealed from the 3.4 Å crystal structure, although a preliminary identification has been made (Kühlbrandt and Wang, 1994).

(3) Future (exciton) calculations on LHC-II aimed at relating the structure to the spectroscopic properties should lead to results that are consistent with the decomposed spectra from the present study, which are characterized by little experimental uncertainty.

MATERIALS AND METHODS

LHC-II was isolated as described in Hemelrijk et al. (1992). Absorption, linear dichroism, and polarized fluorescence measurements were performed as described in the same paper. Polyacrylamide gels for linear dichroism and polarized fluorescence measurements were prepared as in Hemelrijk et al. (1992). The gels were compressed with a factor of 1.25 in both the *x*- and *y*-direction. The corrections of polarized fluorescence spectra for polarization dependent excitation intensity and detection sensitivity will be described at the end of Theory.

Theory

The polarized fluorescence method is based on the theoretical paper by Van Gurp et al. (1988). The complexes are embedded in a polyacrylamide gel that is compressed in the perpendicular *x*- and *y*-directions with an equal factor and expands in the vertical *z*-direction. The compressed gel is placed in a 90° fluorescence setup. Excitation light falls on the sample along the *x* axis, and fluorescence light is detected along the *y* axis. Polarizers in the excitation and detection beam select vertically (V) and horizontally (H) polarized light. Four independent fluorescence intensities at a certain excitation (λ_1) and detection wavelength (λ_2) can be obtained: I_{vv}, I_{vh}, I_{hv}, and I_{hh}, where the subscripts refer to the orientations of the excitation and detection polarizers, respectively. These experimentally accessible observables are related to the parameters S_μ, S_ν G_0, and G_2 (Van Gurp et al., 1988), which depend on the orientation distribution of the molecules in the gel and the orientations of the absorption and emission dipole moment with respect to each other and with respect to the C_3-symmetry axis of the complex, according to

$$I_{vv}(\lambda_1, \lambda_2) = F(\lambda_1, \lambda_2)[1 + 2S_\mu(\lambda_1) + 2S_\nu(\lambda_2) + 4G_0(\lambda_1, \lambda_2)] \quad (1a)$$

$$I_{vh}(\lambda_1, \lambda_2) = F(\lambda_1, \lambda_2)[1 + 2S_\mu(\lambda_1) - S_\nu(\lambda_2) - 2G_0(\lambda_1, \lambda_2)] \quad (1b)$$

$$I_{hv}(\lambda_1, \lambda_2) = F(\lambda_1, \lambda_2)[1 - S_\mu(\lambda_1) + 2S_\nu(\lambda_2) - 2G_0(\lambda_1, \lambda_2)] \quad (1c)$$

$$I_{hh}(\lambda_1, \lambda_2) = F(\lambda_1, \lambda_2)[1 - S_\mu(\lambda_1) - S_\nu(\lambda_2) + G_0(\lambda_1, \lambda_2) - 3G_2(\lambda_1, \lambda_2)]. \quad (1d)$$

$F(\lambda_1, \lambda_2)$ is a parameter that depends on properties of the experimental set-up like the excitation intensity at λ_1 and the detection sensitivity at λ_2, but also on molecular parameters like the absorption at λ_1 and the fluorescence yield at λ_2. In the present study, it serves as a normalization constant.

The equations are based on the fact that I_{ij} is proportional to $\langle(\bar{\mu}\cdot\bar{e}_i)^2(\bar{\nu}\cdot\bar{e}_j)^2\rangle$, where $\bar{\mu}$ and $\bar{\nu}$ are unit vectors along the absorption and emission dipoles and the unit vectors $\bar{e}_i$ and $\bar{e}_j$ denote the orientation of the "excitation" and "detection" polarizers, respectively. For formal definitions of S_μ, S_ν, G_0, and G_2, we refer to Van Gurp et al. (1988). For the specific case of rotationally symmetric particles (like LHC-II) in which rotational equilibration takes place on a time-scale much faster than the fluorescence lifetime (which is in the nanosecond region (Ide et al., 1987), the parameters are given by Van Amerongen et al. (1991)

$$S_\mu = \langle P_2\rangle\langle P_2(\cos\beta_\mu)\rangle \quad (2a)$$

$$S_\nu = \langle P_2\rangle\langle P_2(\cos\beta_\nu)\rangle \quad (2b)$$

$$G_0 = \langle \tfrac{1}{5} + \tfrac{2}{7}\langle P_2\rangle + \tfrac{18}{35}\langle P_4\rangle\rangle\langle P_2(\cos\beta_\mu)\rangle\langle P_2(\cos\beta_\nu)\rangle \quad (2c)$$

$$G_2 = \langle \tfrac{1}{5} - \tfrac{2}{7}\langle P_2\rangle + \tfrac{3}{35}\langle P_4\rangle\rangle\langle P_2(\cos\beta_\mu)\rangle\langle P_2(\cos\beta_\nu)\rangle, \quad (2d)$$

where

$$\langle P_2\rangle = \langle P_2(\cos\beta)\rangle = \langle \tfrac{1}{2}(3\cos^2\beta - 1)\rangle \quad (3a)$$

$$\langle P_4\rangle = \langle P_4(\cos\beta)\rangle = \langle \tfrac{1}{8}(35\cos^4\beta - 30\cos^2\beta + 3)\rangle \quad (3b)$$

are the second and fourth order Legendre polynomials of cos β. The angle β denotes the orientation of the C_3 symmetry-axis (z' axis) of the complex

with respect to the laboratory z-axis. $\langle P_2(\cos \beta_\mu)\rangle$ and $\langle P_2(\cos \beta_\nu)\rangle$ are the second order Legendre polynomials containing the orientation angles of the absorption (β_μ) and emission (β_ν) dipole moments with respect to the z' axis. The brackets denote either averaging over all contributing absorption ($\langle P_2(\cos \beta_\mu)\rangle$) or emission ($\langle P_2(\cos \beta_\nu)\rangle$) dipole moments per trimer or over all contributing trimers ($\langle P_2\rangle$ and $\langle P_4\rangle$). Note that S_μ corresponds to the reduced linear dichroism (see Eq. 8) of all absorption transition dipole moments. It is in order here to elaborate somewhat on the term "rotational equilibration." In the present context, it means that on the average there is no correlation between the orientations of absorption and emission dipole moments around the symmetry axis for a certain combination of excitation and emission wavelengths. As a simple example, we consider the case of three identical pigments a1, a2, and a3, which are symmetry-related around the C_3 axis. Suppose pigment a1 absorbs a photon. If energy transfer between the pigments takes place on a timescale much faster than fluorescence, all pigments have equal probability of emitting a photon and fast rotational equilibration takes place. If for some reason the probability of photon emission by a certain pigment that has also absorbed a photon is larger than for the other two pigments (for instance, because inhomogeneous broadening has led to a significantly red shifted absorption band for this pigment or because the energy transfer process is not much faster than the fluorescence process), then no fast rotational equilibration takes place.

Note that $\langle P_2\rangle$ reflects the degree of orientation of the complexes. For a disc-like complex like trimeric LHC-II $\langle P_2\rangle$ is -0.5 when all complexes are lined up with the trimeric plane parallel to the z-axis. The value of $\langle P_2\rangle$ is 0 when no preferential orientation is present. A priori, no knowledge is available about the value of $\langle P_2\rangle$ apart from the fact that its value should lie between -0.5 and 0 for disc-like particles (Van Amerongen et al., 1991). In an unoriented sample, $\langle P_2\rangle$ and $\langle P_4\rangle$ are equal to 0 and, consequently, $S_\mu = S_\nu = 0$ and $G_0 = G_2 = \frac{1}{5}\langle P_2(\cos \beta_\mu)\rangle\langle P_2(\cos \beta_\nu)\rangle$. The latter parameters are equal to $r/2$, where r is the well known anisotropy parameter, obtained in conventional polarized fluorescence measurements (see also below). In that case

$$I_{vv}(\lambda_1, \lambda_2) = F(\lambda_1, \lambda_2)\,[1 + 2r(\lambda_1, \lambda_2)] \tag{4a}$$

$$I_{vh}(\lambda_1, \lambda_2) = I_{hv}(\lambda_1, \lambda_2) = I_{hh}(\lambda_1, \lambda_2) = F(\lambda_1, \lambda_2)\,[1 - r(\lambda_1, \lambda_2)]. \tag{4b}$$

The latter equations are used to correct for differences in excitation intensities for horizontally and vertically polarized light and for differences in detection sensitivity for horizontally and vertically polarized fluorescence light (see below). The four equations 1a–1d contain five unknowns at a certain combination of λ_1 and λ_2. When excited at a wavelength where $S_\mu = 0$ (which can be determined from the LD spectrum: LD = 0), the emission spectra of I_{vv}, I_{vh}, I_{hv}, and I_{hh} contain only four unknowns and from straightforward combinations of these intensities $S_\nu(\lambda_2)$. $G_0(\lambda_1, \lambda_2)$, $G_2(\lambda_1, \lambda_2)$ and the isotropic fluorescence spectrum $F(\lambda_1, \lambda_2)$ can be extracted. Choosing now a detection wavelength λ_2 where S_ν is well-determined, the spectra $S_\mu(\lambda_1)$, $G_0(\lambda_1, \lambda_2)$, $G_2(\lambda_1, \lambda_2)$, and $F(\lambda_1, \lambda_2)$ can be obtained from the excitation spectra I_{vv}, I_{vh}, I_{hv}, and I_{hh}.

Below, several useful equations are given that can be derived from the equations presented above and that will be used for the interpretation of the results. They hold for rotationally symmetric complexes in which fast rotational equilibration takes place. For nonoriented complexes (isotropic sample) (see, e.g., Van Gurp et al., 1988),

$$r = (I_{vv} - I_{vh})/(I_{vv} + 2I_{vh}) = \tfrac{2}{5}\langle P_2(\cos \beta_\mu)\rangle\langle P_2(\cos \beta_\nu)\rangle. \tag{5}$$

For an oriented sample at an excitation wavelength where $\langle P_2(\cos \beta_\mu)\rangle = 0$ (no LD), S_μ, G_0, and G_2 are all equal to zero and the following equations hold:

$$(I_{vv} - I_{vh})/(I_{vv} + 2I_{vh}) = (I_{hv} - I_{hh})/(I_{hv} + 2I_{hh}) = S_\nu. \tag{6}$$

$\langle P_2\rangle$ can be obtained from

$$(G_0 - 6G_2)/(S_\mu S_\nu) = (-1 + 2\langle P_2\rangle)/\langle P_2\rangle^2. \tag{7}$$

To obtain the intensities I_{vv}, I_{vh}, I_{hv}, and I_{hh} as given in Eqs. 1a–1d, one has to correct for differences in excitation intensity and detection sensitivity that depend on the polarization direction. For an unoriented sample, the ratio of detection sensitivities for vertically and horizontally polarized light is given by I'_{hv}/I'_{hh} because I_{hv} and I_{hh} should be equal (Eq. 4b). The primes denote measured intensities as opposed to the corrected intensities, which do not carry a prime. Therefore, $I_{vh} = I'_{vh}\,C_1$ ($C_1 = I'_{hv}/I'_{hh}$). Because $I_{vh} = I_{hv} = I_{hh}$, one can obtain I_{hv} according to $I_{hv} = I'_{hv}\,C_2$ (where $C_2 = I'_{vh}/I'_{hh}$) and $I_{hh} = I'_{hh}\,C_3$ (where $C_3 = I'_{vh}\,I'_{hv}/I'_{hh}\,I'_{hh}$). The same correction factors C_1, C_2, and C_3 obtained from the isotropic sample can then be used for the correction of the intensities obtained for the oriented sample.

For linear dichroism, the following relation holds (see, e.g., Van Gurp et al. 1988):

$$\Delta A/3A = \langle P_2\rangle\langle P_2(\cos \beta_\mu)\rangle, \tag{8}$$

where ΔA is the difference in absorption for vertically and horizontally polarized light and A is the isotropic absorption, which can be obtained for an uncompressed gel (corrected to same concentration and optical pathlength). $\Delta A/3A$ is called the reduced linear dichroism.

RESULTS

In Fig. 1 *A*, the 77 K absorption A (*solid line*) and LD (ΔA) (*dashed line*) spectra of trimeric LHC-II in the Q_y region are given. The spectra are similar to those given by Hemelrijk et al. (1992), although the shoulders near 661 and 670 nm are less pronounced in the present case. The reduced linear dichroism spectrum $\Delta A/3A$ is given in Fig. 1 *B*. Noteworthy is the slight drop of the reduced LD at the red edge (above 680 nm) to a value of about 85 ± 5% of the peak value. Despite the fact that this drop occurs in a region of low absorption and a steep slope in the A and ΔA spectra (which can cause increased uncertainty in the values of $\Delta A/3A$), it turns out to be very reproducible (measured 3 times). It shows that absorption transition dipoles causing the red-most absorption have a slightly different orientation (more out of the plane of the trimer) than the transition dipole moments in the peak around 676 nm. This point is important because the fluorescence at 77 K and below is expected to originate for a significant part from the red-most states. The reduced LD is not plotted above 685 nm because the corresponding values are subject to a large uncertainty because the absorption values (present in the denominator of the expression for reduced LD) are close to zero above this wavelength. The influence of uncertainties in the baseline corrections, therefore, become prominent.

Essential for the further analysis of the polarized absorption and fluorescence data is that 1) rotational excitation equilibration (and, therefore, depolarization) occurs on a time scale much shorter than the fluorescence lifetime, and 2) that unconnected (free) chlorophyll does not significantly contribute to the fluorescence. It has already been argued in the introduction that the rotational equilibration is sufficiently fast. The absence of free chlorophyll has to be checked independently. If both conditions hold, then the observed anisotropy $r = \frac{2}{5}\langle P_2(\cos \beta_\mu)\rangle\,\langle P_2(\cos \beta_\nu)\rangle$ for the isotropic sample should be zero at all emission wavelengths upon excitation at 659 nm where $\Delta A = 0$ ($\langle P_2(\cos \beta_\mu)\rangle = 0$) (see Eq. 5). In Fig. 2 *A*, it is shown that the anisotropy curve is essentially zero at all emission wavelengths. The results become noisier upon going to longer wavelengths because

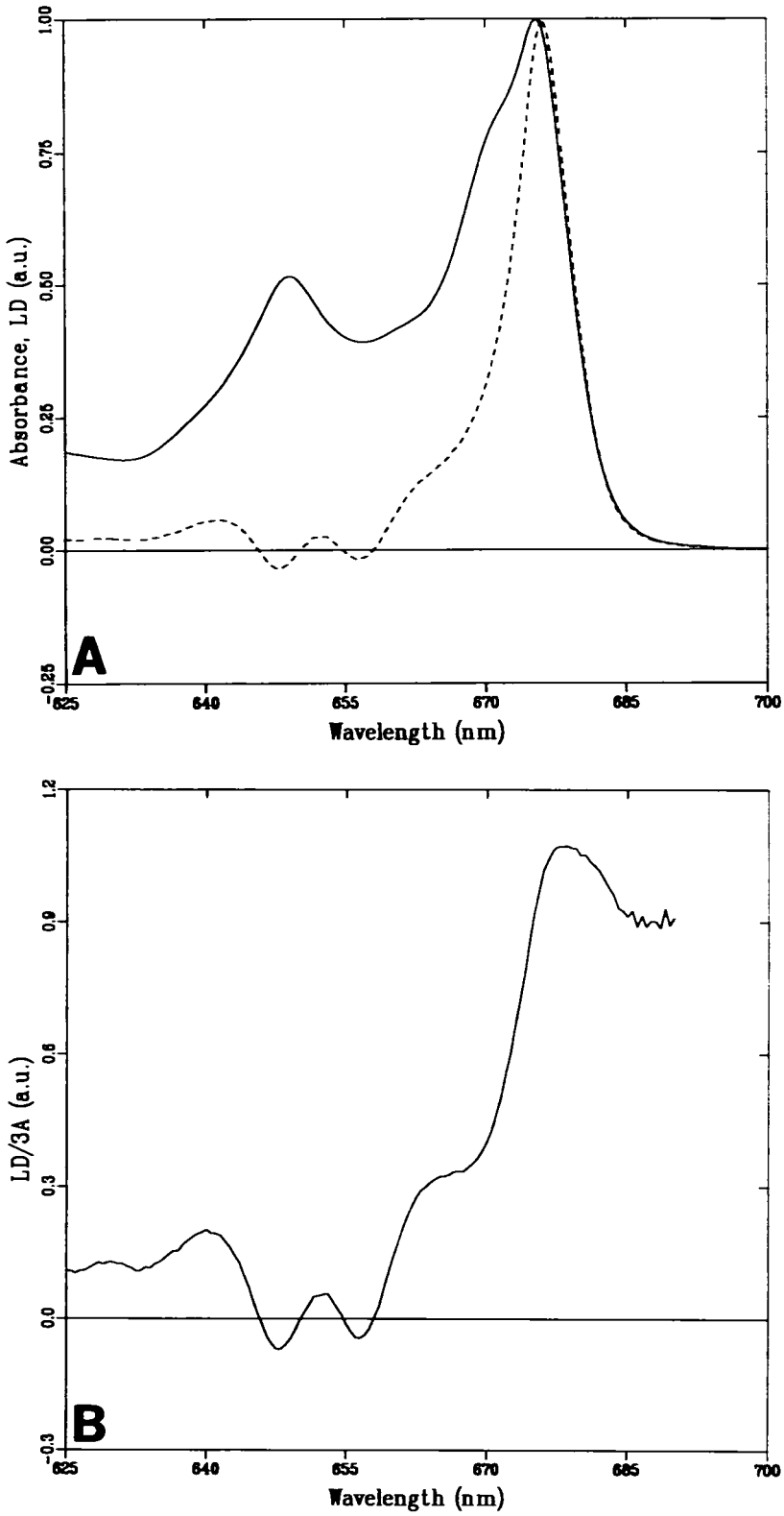

FIGURE 1 (*A*) (——) Absorption of unoriented and (- - - -) linear dichroism of oriented LHC-II at 77 K obtained with an optical bandwidth of 1.5 nm. The spectra have been normalized in the peaks. (*B*) $A/\Delta A$ spectrum of LHC-II obtained from the spectra in *A*.

the fluorescence yield decreases as is shown in the same figure. For some old samples, it turned out (results not shown) that the anisotropy was higher than 0 at all emission wavelengths upon excitation at 659 nm with especially large values of $r(>0.2)$ near 670 nm, where the fluorescence of free chlorophyll dominates (Kwa et al., 1994). This demonstrates that disturbing effects of unconnected chlorophylls are easily detected, and their presence could be ruled out in the present case.

Fig. 2 *B* shows the excitation anisotropy spectrum $r(\lambda_1)$ recorded on the same (unoriented) sample at 77 K with an optical bandwidth of 6 nm. The detection wavelength

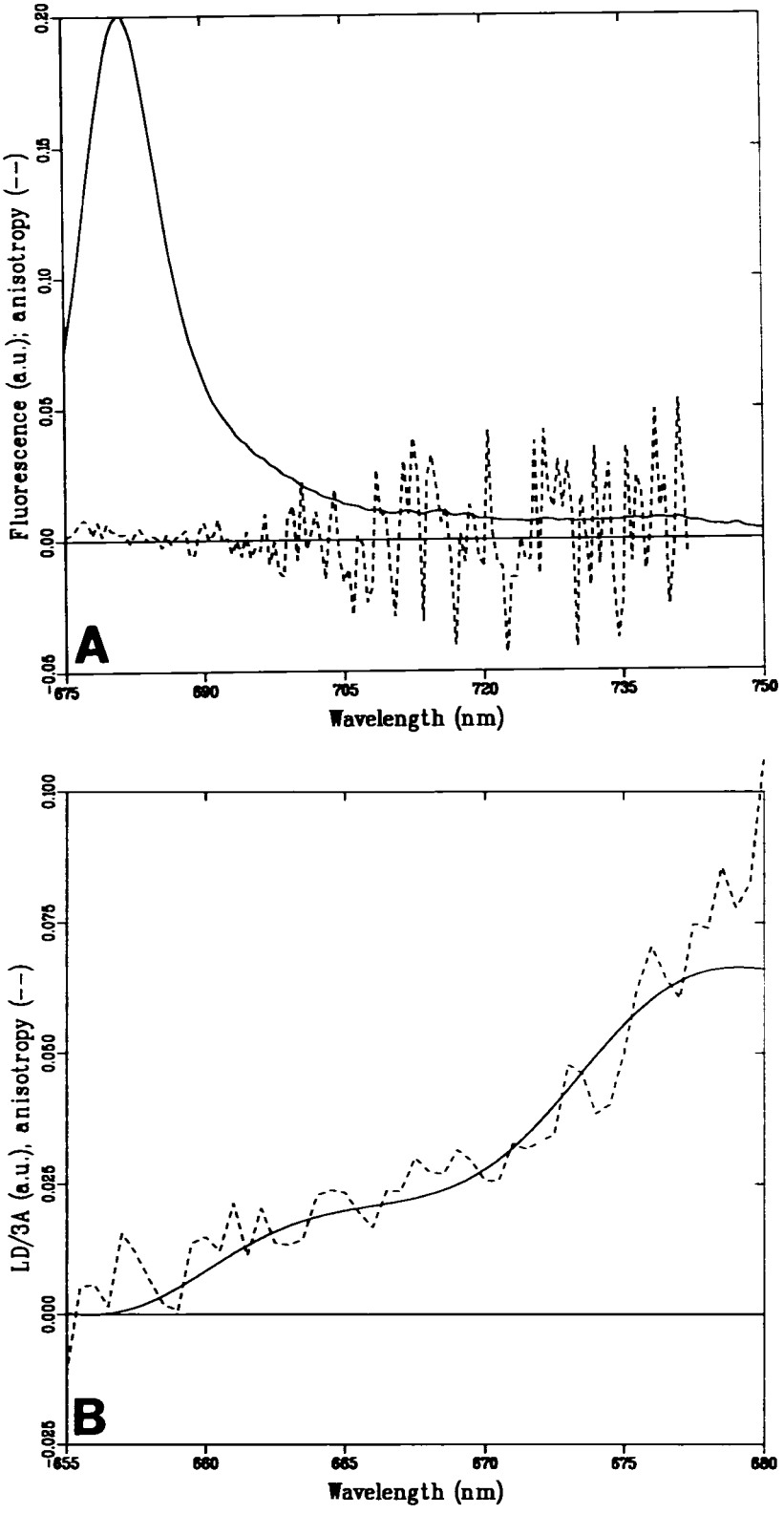

FIGURE 2 (*A*) Fluorescence anisotropy of unoriented LHC-II at 77 K obtained with an optical bandwidth of 6 nm in the detection and 3 nm in the excitation branch. The excitation wavelength was 659 nm. (*B*) (——) Reduced linear dichroism spectrum of oriented LHC-II at 77 K, obtained with an optical bandwidth of 6 nm and normalized to the anisotropy spectrum in the wavelength region 665–675 nm. (- - - -) Excitation anisotropy spectrum of unoriented LHC-II at 77 K, obtained with an optical bandwidth of 6 nm. Detection was performed at 692 nm with an optical bandwidth of 6 nm.

was 692 nm. The spectrum is very similar to the one presented by Hemelrijk et al. (1992) detected at 740 nm. Note that in Hemelrijk et al. (1992) the polarization P is given instead of the anisotropy. The shape of $r(\lambda_1)$ ($= \frac{2}{5}\langle P_2(\cos\beta_\mu(\lambda_1))\rangle\langle P_2(\cos\beta_e)\rangle$) is expected to be the same as that of the reduced LD spectrum ($\langle P_2\rangle \cdot \langle P_2(\cos\beta_\mu(\lambda))\rangle$). In Fig. 2 *B* it is shown that only above 676 nm the spectra start to deviate from each other, indicating that complete rotational equilibration does not take place anymore beyond this wavelength. However, by imposing the

shape of the reduced LD on the anisotropy spectrum, it can be calculated what r would have been at 678 nm (the maximum of the reduced LD) if rotational equilibration would have taken place, namely, $r = 0.068 \pm 0.006$. This corresponds to a value of $\langle P_2(\cos \beta_\mu)\rangle/\langle P_2(\cos \beta_\nu)\rangle = 0.170 \pm 0.015$ in the peak of the reduced LD (678 nm). Additional measurements on oriented complexes are now needed to determine the individual parameters $\langle P_2(\cos \beta_\mu(\lambda))\rangle$ and $\langle P_2(\cos \beta_\nu)\rangle$.

In Fig. 3 *A*, $(I_{vv} - I_{vh})/(I_{vv} + 2I_{vh})$ and $(I_{hv} - I_{hh})/(I_{hv} + 2I_{hh})$ obtained upon 659 nm excitation of an oriented sample

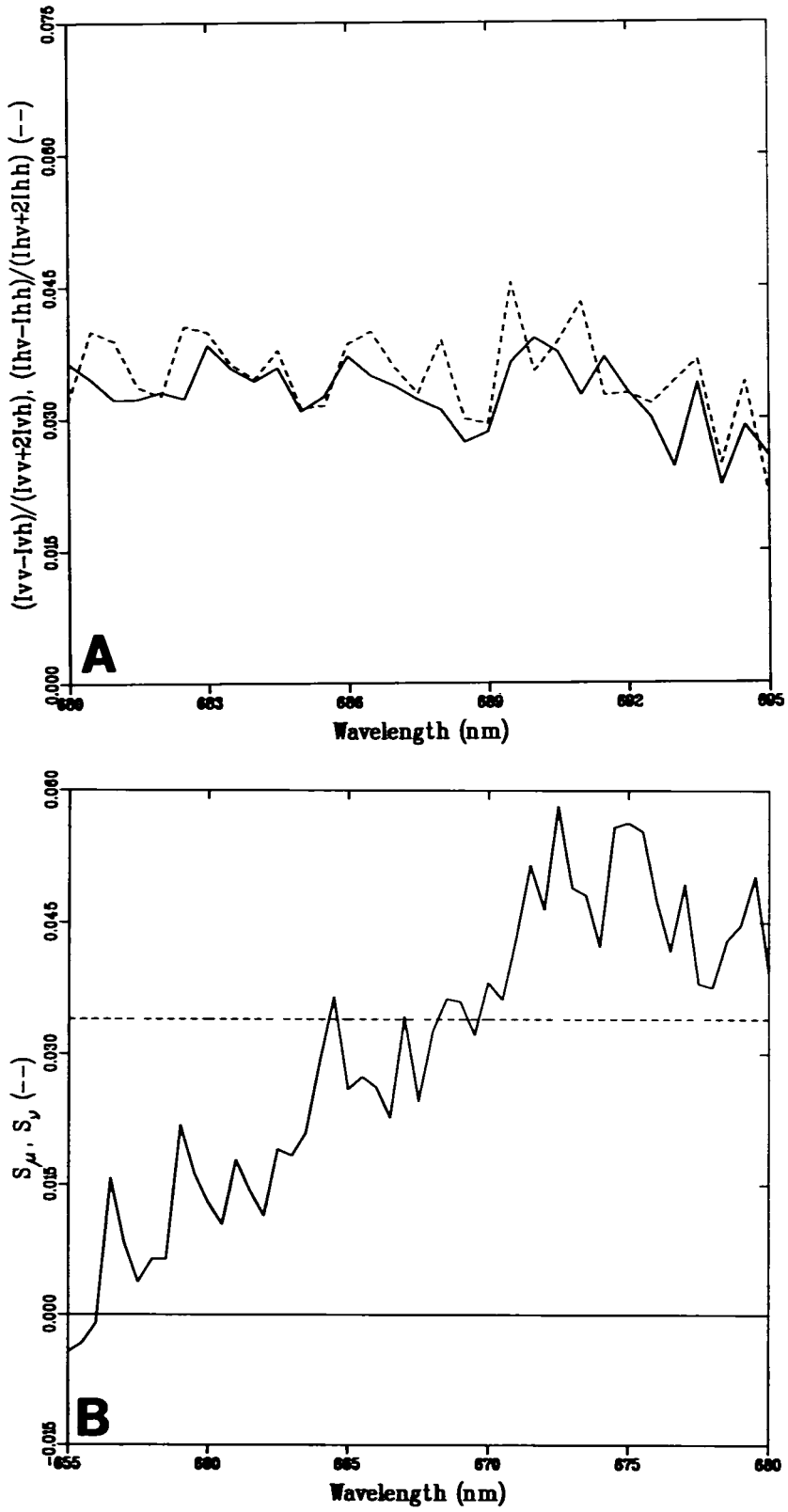

FIGURE 3 (*A*) (——) $(I_{vv} - I_{vh})/(I_{vv} + 2I_{vh})$ and (- - - -) $(I_{hv} - I_{hh})/(I_{hv} + 2I_{hh})$ of LHC-II oriented in a compressed gel at 77 K, obtained with an optical bandwidth of 6 nm in the detection branch after excitation at 659 nm with an optical bandwidth of 3 nm. (*B*) (——) S_μ (77 K) obtained on the same sample as used for *A*. Fluorescence was detected at 692 nm with an optical bandwidth of 6 nm. The band width for the excitation wavelength was 6 nm. S_μ was obtained as described in the text. (- - - -) The value of $S_\nu = 0.34$ as obtained from *A*.

are plotted. For LHC-II trimers in the absence of detached chlorophyll, both parameters are expected to be identical to each other at all emission wavelengths and equal to S_ν (see Eq. 6). It is indeed observed that the parameters are equal to each other at all wavelengths. Moreover, S_ν does not depend on the emission wavelength. Its average value is 0.034 ± 0.001 between 680 and 695 nm, where the fluorescence is most intense and, thus, the results are most reliable. However, even for detection wavelengths up to 750 nm, very similar values are obtained (not shown).

From the excitation spectra I_{vv}, I_{vh}, I_{hv}, and I_{hh}, S_μ was obtained using S_ν = 0.034 and making use of equations 1a–1d (Fig. 3 *B*). In the same figure, the value of S_ν is indicated by the straight horizontal line. The value of S_μ around 676 nm is larger than that of S_ν. For the further analysis, it is important to establish a lower limit for $S_\mu(678\text{ nm})/S_\nu = \langle P_2(\cos\beta_\mu(678\text{ nm}))\rangle/\langle P_2(\cos\beta_\nu)\rangle$ (note that at 678 nm, the peak of the reduced dichroism occurs). The experiment was repeated 3 times, and an absolute lower value of 1.20 was determined. With the above given value of $\langle P_2(\cos\beta_\mu(678\text{ nm}))\rangle/\langle P_2(\cos\beta_\nu)\rangle = 0.170 \pm 0.015$, one can now calculate that the value of $\langle P_2(\cos\beta_\mu(678\text{ nm}))$ lies between −0.43 and −0.50 (where use has been made of the fact that the theoretical minimum for the second order Legendre polynomial is −0.50) and $\langle P_2(\cos\beta_\nu)\rangle = -0.34 \pm 0.03$ (wavelength-independent). The value of $\langle P_2(\cos\beta_\mu)\rangle$ was determined with a spectral bandwidth of 6 nm. This leads to a flattening of the reduced LD spectrum (which is also the reason that small differences exist between the reduced LD spectra in Figs. 1 *B* and 2 *B*). It turns out that the peak value of $\Delta A/3A$ increases by 3% when a resolution of 1.5 nm is used, leading to $\langle P_2(\cos\beta_\mu(678\text{ nm}))\rangle = -0.47 \pm 0.03$. In principle, both order parameters $\langle P_2(\cos\beta_\mu)\rangle$ and $\langle P_2(\cos\beta_\nu)\rangle$ could also be positive, but the negative solution has to be taken because the trimers are known to be approximately disc-like (Kühlbrandt and Wang, 1991) and, in that case, negative values for $\langle P_2\rangle$ are expected (Van Amerongen et al., 1991; Ganago et al., 1980).

The analysis of the above experiments was based on a combined use of LD and polarized fluorescence measurements on oriented and unoriented samples. We have also obtained $\langle P_2(\cos\beta_\mu)\rangle$ and $\langle P_2(\cos\beta_\nu)\rangle$ in a different way using only polarized fluorescence measurements on a compressed sample. In principle, the analysis could have been done with results of the compressed sample given above, but the results turned out to be too noisy to be meaningful for this type of analysis. A different set of data on another sample was used for this goal. The detection wavelength was chosen to be 740 nm, and a bandwidth of 18 nm was used. The value of S_ν was obtained as outlined above and was 0.046 ± 0.001 in this specific case. With the use of this value, S_μ, G_0, and G_2 were determined. In Fig. 4, S_μ, G_0, and G_2 are given after normalization between 665 and 675 nm. The shape of all spectra is very similar, as expected for trimeric LHC-II (Eq. 2), and $G_0 = (1.17 \pm 0.02)S_\mu$ and $G_2 = (1.15 \pm 0.02)S_\mu$. No significant deviation from rotational equilibration can be observed in the given wavelength region. Some deviation was observed upon excitation above 676 nm and detection at 692 nm (see above), but because the analysis for both types of analysis was restricted to the wavelength region below

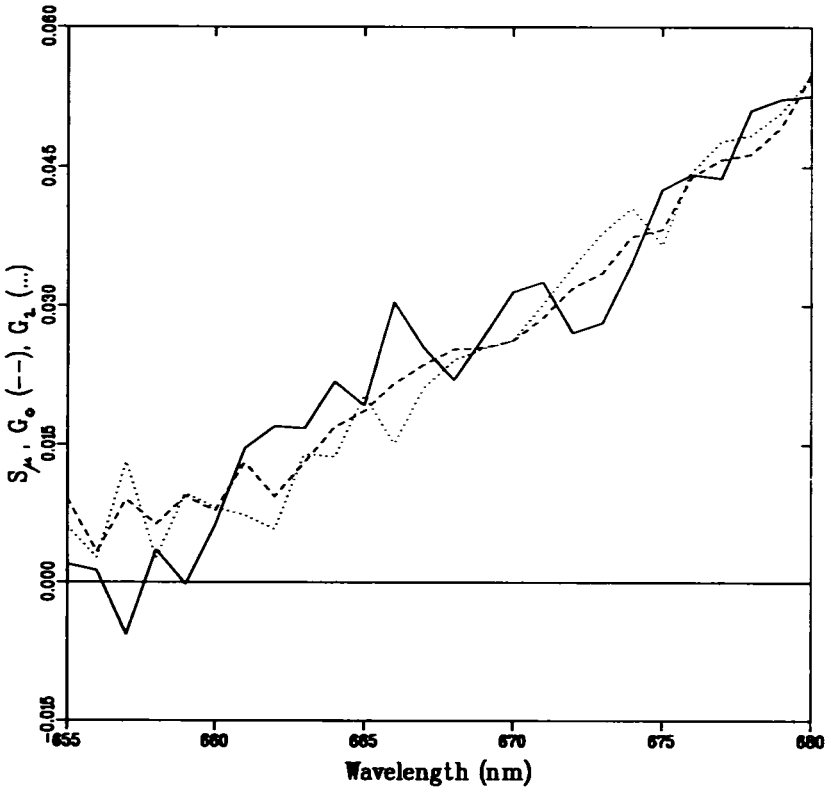

FIGURE 4 (——) S_μ, (- - - -) G_0, and (·····) G_2 of LHC-II at 77 K in a compressed gel. Detection wavelength is 740 nm with an optical bandwidth of 18 nm. The curves have been calculated as described in the text with a value of S_ν = 0.046. The optical bandwidth of the excitation light was 6 nm. G_0 and G_2 have been normalized to S_μ between 665 and 675 nm by multiplying them with 1.17 and 1.15, respectively.

676 nm, the possible absence of rotational equilibration above 676 nm does not influence the analysis in both cases. The value of $\langle P_2 \rangle$ is determined from $(G_0 - 6G_2)/(S_\mu S_\nu) = (-1 + 2\langle P_2 \rangle)/\langle P_2 \rangle^2 = -95 \pm 5$. From this, it is calculated that $\langle P_2 \rangle = 0.093 \pm 0.003$ or $\langle P_2 \rangle = -0.114 \pm 0.004$. Again, the negative solution is taken. This leads to a value of $\langle P_2(\cos \beta_\mu(678 \text{ nm})) \rangle = -0.47 \pm 0.03$ after correction for the optical bandwidth (see above) and $\langle P_2(\cos \beta_\nu) \rangle = -0.40 \pm 0.03$, and especially the first value is in good agreement with the value presented above. In Table 1, the values of $\langle P_2(\cos \beta_\mu) \rangle$ are given at different wavelengths.

DISCUSSION

The main role of LHC-II is to absorb sunlight and effectively transfer the induced excitation energy to the reaction center of (merely) Photosystem II. To get a detailed understanding of both processes, a detailed correlation between the structure (Kühlbrandt and Wang, 1994) and the spectroscopy is needed. Although a wealth of time-resolved and steady-state spectroscopic information has been gathered over the last years (Hemelrijk et al., 1992; Kwa et al., 1992a, b; Gillbro et al., 1985; Eads et al., 1989; Savikhin et al., 1994; Ide et al., 1987; Reddy et al., 1994), such a correlation is by no means obvious. To understand the dynamic processes in LHC-II, which depend on the excited state properties and the orientations and positions of pigments and their transition dipole moments with respect to each other, a detailed understanding of the absorption spectrum and knowledge of the polarization of the absorption bands is needed.

At least 36 pigments per trimer contribute to the absorption spectrum in a narrow wavelength region (Hemelrijk et al., 1992; Kwa et al., 1992a). These pigments interact with the protein matrix in a way that is not fully understood that influences the composition of the absorption spectrum and the kinetics of the various transfer processes. For instance, the absorption spectrum can shift (with respect to the spectrum in vacuum) because of the presence of charged or polar amino acids in the direct environment of a pigment (Eccles and Honig, 1983) or because of the average dielectric constant of the surroundings (Renge, 1992). Moreover, the glass-like nature of the protein does lead to inhomogeneous broadening of absorption bands and, therefore, even pigments on identical positions of various trimers do have varying absorption characteristics. Finally, the pigment-protein coupling leads to phonon side-bands. The impact of these types of interactions cannot be directly deduced from the crystal structure, and different approaches are needed to establish their effects.

TABLE 1 Average dipole orientations

Wavelength ⟨(nm)⟩	$\langle P_2(\cos \beta_\mu(\lambda)) \rangle$
685	−0.39
678	−0.47
670	−0.18
661	−0.08
656	+0.02
652	−0.02
647.5	+0.03
640	−0.09

Values of $\langle P_2(\cos \beta_\mu(\lambda)) \rangle$ at different wavelengths obtained from Fig. 1 *B*, taking $\langle P_2(\cos \beta_\mu(678 \text{ nm})) \rangle = -0.47$.

The pigments interact with each other through excitonic coupling, and this will influence the absorption spectrum substantially. Although excitonic calculations can be performed for well defined geometries and energy levels, this is not possible for LHC-II yet because of the uncertainty in the energy levels (see above) and the unknown orientations of the transition dipole moments of individual pigments, and this precludes detailed excitonic calculations in a straightforward way. Although in the latest paper on the crystal structure of LHC-II (Kühlbrandt and Wang, 1994) the identities of all chlorophylls (Chl *a* and Chl *b*) were assigned, this assignment is not conclusive yet.

Summarizing, at this stage a detailed comparison of the absorption spectrum with the structure of LHC-II is impossible. An essential step in elucidating the correlation is the determination of the absorption spectra parallel and perpendicular to the C_3-symmetry axis of the trimer. Any assignment of pigments to be either Chl *a* or Chl *b* should be in accordance with the average orientations of the Q_y transition dipole moments obtained in this study, and calculated spectra after such an assignment should not only be in accordance with the isotropic absorption spectrum but also with the "parallel" and "perpendicular" spectra.

It was shown above that accurate information about the orientations of absorption and emission transition dipole moments in LHC-II can be obtained with respect to the symmetry axis, provided that the following conditions hold:

(1) Rotational equilibration within the trimer takes place, and the rotational equilibration time is much faster than the fluorescence lifetime (excited state lifetime).
(2) No free chlorophyll is present in the samples.

It was argued in the introduction that the first condition is fulfilled for LHC-II. The second condition was also fulfilled in the present study, as was shown in Results. The latter condition turned out not to be true for some older samples, but it could easily be detected. Finally, the good agreement between the values of $\langle P_2(\cos \beta_\mu) \rangle$ obtained from two essentially different experimental approaches indicates the correctness of the assumptions. Therefore, we are confident about the obtained values $\langle P_2(\cos \beta_\mu(678 \text{ nm})) \rangle = -0.47 \pm 0.03$, $\langle P_2(\cos \beta_\nu(692 \text{ nm})) \rangle = -0.34 \pm 0.03$ and $\langle P_2(\cos \beta_\nu(740 \text{ nm})) \rangle = -0.40 \pm 0.03$.

Emitting dipole moments

The finding that the emission dipole moments are somewhat further out of plane than the absorption dipole moments of the 676-nm band is in agreement with the fact that the reduced LD spectrum drops at the red side of the absorption maximum. At 77 K, the emission arises from several states (Kwa et al., 1992a). These correspond to the red part of the

absorption spectrum (>676 nm) at 77 K because of thermal equilibration. In this wavelength region, the average value of the reduced LD (and, therefore, S_μ) is less than that in the maximum, the lower value of S_μ can be anticipated provided that the absorption and emission dipole moments for a specific state are approximately parallel. For isolated Chl *a*, it was indeed found that the Q_y absorption and emission dipole moments are parallel within 10° (Van Gurp et al., 1989). The value of S_μ is more or less independent of the detection wavelength, which is expected in a homodisperse sample of LHC-II. In previous measurements (Kwa et al., 1992a), significant variations in S_μ were present, which we now ascribe to the presence of detached chlorophyll and aggregates of LHC-II.

Absorption parallel and perpendicular to the plane of the trimer

We will now proceed with a decomposition of the absorption spectrum into components parallel and perpendicular to the symmetry axis. First, $A_\parallel$ and $A_\perp$ are defined as the absorption parallel and perpendicular to the C_3-symmetry axis, respectively. A is again the isotropic absorption. The following equations hold:

$$A(\lambda) = \tfrac{1}{3}(A_\parallel(\lambda) + 2A_\perp(\lambda)) \quad (9)$$

$$A_\parallel(\lambda) - A_\perp(\lambda) = 3\langle P_2(\cos\beta_\mu)\rangle A(\lambda). \quad (10)$$

A is simply the average of the absorption spectra along three perpendicular axes, which can be chosen parallel and perpendicular (twice) to the symmetry axis. The spectra $A_\parallel(\lambda)$ and $A_\perp(\lambda)$ can now be determined according to

$$A_\parallel(\lambda) = (1 + 2\langle P_2(\cos\beta_\mu(\lambda))\rangle A(\lambda) \quad (11)$$

$$A_\perp(\lambda) = (1 - \langle P_2(\cos\beta_\mu(\lambda))\rangle A(\lambda). \quad (12)$$

The resulting spectra are presented in Fig. 5 for the extreme values of −0.44 and −0.50 for $\langle P_2(\cos\beta_\mu(\lambda))\rangle$ in the maximum of the reduced LD. Below, we will give a discussion of the average orientation of the dipole moments of different bands for which it was possible to (partly) resolve them in the absorption spectrum. As was discussed above, there is extensive overlap of many bands, which precludes a detailed analysis of the LD of each individual absorption band.

Chlorophyll *a*

676-nm band

Probably the most striking feature of the decomposed spectra is the fact that the 676-nm band hardly shows up in $A_\parallel$, i.e., the corresponding dipole moments are oriented almost perfectly parallel to the plane of the trimer. The dipoles are exactly in-plane if $\langle P_2(\cos\beta_\mu(678\text{ nm}))\rangle = -0.50$. In case $\langle P_2(\cos\beta_\mu(678\text{ nm}))\rangle = -0.44$, the average angle between the dipoles and the plane is between 12° and 8°. The fact that 1) this band corresponds to a large dipole strength, 2) the corresponding dipole orientations are well known now, and 3) the fact that a similar band is also present in other homologous pigment-protein complexes that differ in other parts of the absorption spectrum (Jennings et al., 1993) makes the 676-nm band a possible key band for future iden-

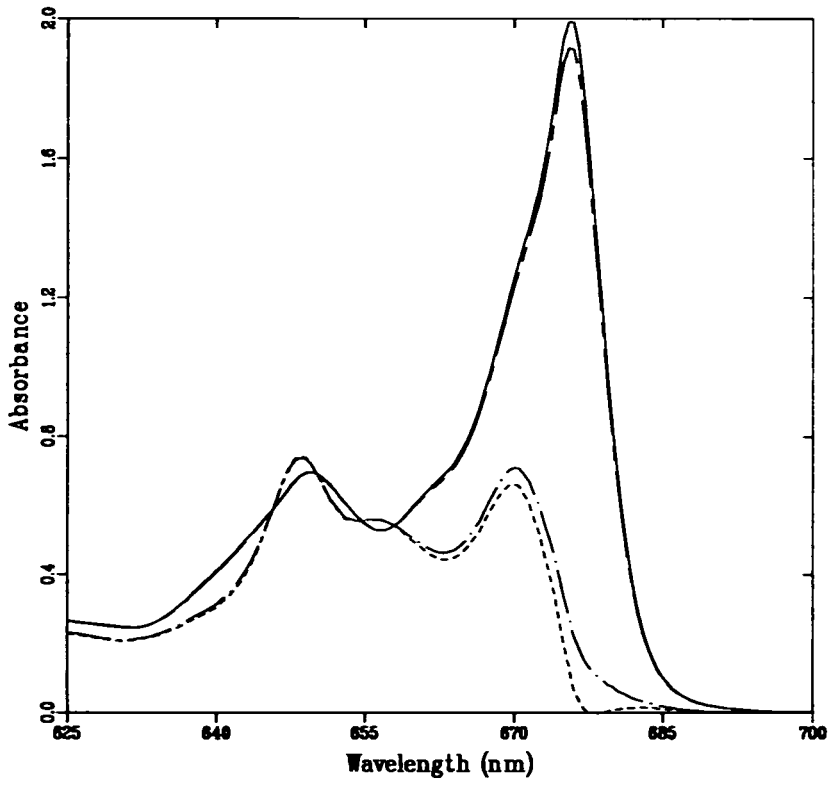

FIGURE 5 (——, - - - -) Absorption spectrum of LHC-II at 77 K along an arbitrary vector perpendicular to the symmetry axis and (- - - -, – – –) parallel to it. These spectra were obtained as described in the text. The spectra were calculated from Fig. 1 *A* using a value of $\langle P_2(\cos\beta_\mu(678\text{ nm}))\rangle = -0.5$ (——, - - - -) or $\langle P_2(\cos\beta_\mu)\rangle = -0.44$ (- - - -, – – – –), which represent extreme values of the parameter $\langle P_2(\cos\beta_\mu)\rangle$ as described in the text.

tification of the corresponding pigments in the crystal structure that make up a large fraction of the total amount of pigments.

680-nm band

The value of $\langle P_2(\cos \beta_\mu(685 \text{ nm}))\rangle$ is between -0.42 and -0.37 (corresponding to an angle between 13° and 17° out of plane if all contributing dipoles have the same orientation with respect to the C_3 axis). This value is similar to that obtained for $\langle P_2(\cos \beta_\mu(692 \text{ nm}))\rangle$, which is -0.34 ± 0.03. As was already discussed above, this similarity is expected because the fluorescence arises mainly from the lower energy states. It has been demonstrated recently that at 4 K the fluorescence arises from a low energy state near 680 nm, hidden under the main 676 nm absorption profile (Reddy et al., 1994).

The present study confirms this finding at 77 K. Because the absorption bands broaden at higher temperatures, there will be more overlap between the 676- and the 680-nm bands at 77 K than at 4 K. This is probably the reason that only above 684 nm the reduced LD spectrum is flat, i.e., no contribution of the broadened 676-nm band is present. However, it cannot be ruled out that the lower energy band is somewhat more red-shifted at 77 K, which would be in agreement with the Gaussian decomposition of the absorption spectrum of LHC-II from pea at 77 K (Zucchelli et al., 1990), showing a low intensity band near 683 nm. At somewhat shorter wavelengths, the 676-nm band probably overlaps with the 680-nm band, leading to higher reduced LD values.

670-nm band

$A_\parallel$ is dominated in the Chl *a* region by a band around 670 nm. For $A_\perp$, the contribution of this band is harder to quantify because the 676 nm absorption band dominates. Assuming that the 676 nm band has a symmetric shape and subtracting it from the total spectrum allows an estimation of the contribution of the 670-nm band to $A_\perp$. This leads to a value of $\langle P_2(\cos \beta_\mu)\rangle = -0.1 \pm 0.05$ for the 670-nm band, corresponding to an angle of 31° ± 2° with the plane if all dipole moments that contribute to the 670-nm band have the same orientation β_μ. If there is a distribution of orientations, then the average value for the angle β_μ does decrease because different angles are weighted differently in the average value of $\langle P_2(\cos \beta_\mu)\rangle$. A lower limit for the average angle with the plane is 22°. Because the 676-nm band must be asymmetrically broadened towards the blue because of vibrations and phonons that couple to the electronic transitions, the estimated contribution of the 670-nm band to $A_\perp$ should be considered as an upper limit, and the average angle with the plane must be larger. We estimate the upper limit to be 38°. In summary, the average angle between the "670-nm" dipoles and the plane of the trimer is 30° ± 8°. One should keep in mind that the 670-nm band is composed of at least three sub-bands with maxima near 668, 671, and 673 nm (Hemelrijk et al., 1992; S. Nußberger, J. P. Dekker, W. Kühlbrandt, B. M. van Bolhuis, R. van Grondelle, and H. van Amerongen, unpublished data).

661-nm band

For the band near 661 nm in the Chl *a* region, $\langle P_2(\cos \beta_\mu)\rangle$ is estimated to be -0.15 ± 0.1. Again, we want to stress that there are more than one (possibly weak) absorbing species contributing to the peak at 661 nm. For instance, $A_\parallel$ shows significant absorption near this wavelength without a distinct shoulder at 661 nm, in contrast to $A_\perp$, which shows a clear peak. In trying to understand the spectroscopy of LHC-II, one should appreciate that there are probably many (excitonic) bands present in the absorption spectrum that overlap each other to a significant extent. For instance, monomeric LHC-II can be obtained (S. Nußberger, J. P. Dekker, W. Kühlbrandt, B. M. van Bolhuis, R. van Grondelle, and H. van Amerongen, unpublished data) that does not show a distinct absorption band at 661 nm but nevertheless gives rise to a similar bump in the LD spectrum above 660 nm, as observed for trimeric LHC-II.

Using the spectra $A_\parallel$ and $A_\perp$, the average angle between all Q_y transition dipole moments of Chl *a* and the trimeric plane can be calculated. In LHC-II, the pigments are closely packed (Kühlbrandt and Wang, 1991), which leads unavoidably to strong excitonic interactions. Therefore, the different absorption bands should not be considered as corresponding to individual pigments but to collective excitations of different pigments. The associated transition dipole moments then also correspond to delocalized excitations and do not directly refer to the original directions of the Q_y transition dipole moments of individual pigments. However, the average orientations of the excitonic dipole moments with respect to the symmetry axis, weighted by the corresponding dipole strength (absorption intensity) should be equal to the average orientation of the individual Q_y dipoles, according to simple exciton theory. Stated more quantitatively,

$$\sum |\mu_i|^2 \langle P_2(\cos \beta_\mu(i))\rangle = \sum |\mu_j|^2 \langle P_2(\cos \beta_\mu(j))\rangle.$$

Here i corresponds to the different excitonic transitions, whereas j corresponds to the individual pigments. By somewhat arbitrarily dividing the absorption spectrum into a Chl *a* region above 660 nm and a Chl *b* region below 660 nm (S. Nußberger, J. P. Dekker, W. Kühlbrandt, B. M. van Bolhuis, R. van Grondelle, and H. van Amerongen, unpublished data), it can be concluded that the average angle between the monomeric Chl *a* Q_y transition dipole moments and the trimeric plane is 15°–20°. Choosing the boundary several nanometers to the red or to the blue of 660 nm hardly affects the calculated value of the average angle.

Chlorophyll *b*

656-nm band

The Chl *b* region shows several distinct spectral features. Around 656 nm, there is a clearly resolved band in the out-of-plane spectrum that is not visible in the in-plane spectrum. Therefore, the total absorption around 656 nm contains sig-

nificant contributions from bands not centered at this wavelength. It is possible that strongly blue-shifted 0-0 transitions of Chl *a*, arising from strong Chl *a*-Chl *a* interactions absorb near 656 nm, but also Chl *b* bands could contribute. The value of $\langle P_2(\cos \beta_\mu) \rangle$ is 0.02 at 656 nm.

649-nm band

At 649.5 nm, a sign change is observed in the LD spectrum, with the high energy dipole moments more out of plane than the low energy dipoles. At least three bands absorb around 649 nm, namely, near 647, 649, and 652 nm, and they overlap considerably (S. Nußberger, J. P. Dekker, W. Kühlbrandt, B. M. van Bolhuis, R. van Grondelle, and H. van Amerongen, unpublished data). This makes it difficult to get detailed information about the absorption intensities of the different bands parallel and perpendicular to the trimeric plane.

640-nm band

Finally, there is a band near 640 nm, and the value of $\langle P_2(\cos \beta_\mu) \rangle$ at this wavelength is -0.09. At this wavelength, there is some Chl *a* contribution (from both Q_x and vibronic Q_y bands with opposite LD), but it does not significantly influence the reduced LD.

The average absorption intensity in the Chl *b* region is about equal along the C_3 axis and any perpendicular axis, unlike what is observed in the Chl *a* region, and it implies an average angle between the dipole moments and the trimeric plane close to 35°.

Future studies will be directed at relating the spectroscopic properties to the crystal structure. In view of the complexity of LHC-II, it is important that it is possible to obtain reconstituted LHC-II after over-expression of the protein in *E. coli* (see, e.g., Paulsen et al., 1993). This offers the possibility of selectively modifying chlorophyll binding sites that have been identified in the 3.4 Å crystal structure (Kühlbrandt and Wang, 1994), which then can lead to a direct correlation between the identity of the specific pigments, their contributions to the absorption spectrum, and the orientations of their dipole moments.

The authors are indebted to Florentine Calkoen for isolating LHC-II. Dr. Jan. P. Dekker is acknowledged for careful reading the first version of the manuscript and for useful discussions.

This research was supported by the Dutch Foundation for Biophysics (SvB) and financed by the Netherlands Organization for Scientific Research (NWO).

REFERENCES

Eads, D. E., E. W. Castner, R. S. Alberte, L. Mets, and G. R. Fleming. 1989. Direct observation of energy transfer in a photosynthetic membrane: chlorophyll *b* to chlorophyll *a* transfer in LHC. *J. Phys. Chem.* 93:8271–8275.

Eccles, J., and B. Honig. 1983. Charged amino acids as spectroscopic determinants for chlorophyll *in vivo*. *Proc. Natl. Acad. Sci. USA.* 80: 4959–4962.

Ganago, A. O., M. V. Fok, I. A. Abdourakhmanov, A. A. Solov'ev, and Yu. E. Erokhin. 1980. Analysis of the linear dichroism of reaction centers oriented in polyacrylamide gels. *Mol. Biol. (Mosc.).* 14:381–389.

Gillbro, T., V. Sundström, A. Sandström, M. Spangfort, and B. Andersson. 1985. Energy transfer within the isolated light-harvesting chlorophyll *a/b* protein of photosystem II (LHC-II). *FEBS Lett.* 193:267–270.

Hemelrijk, P. W., S. L. S. Kwa, R. van Grondelle, and J. P. Dekker. 1992. Spectroscopic properties of LHC-II, the main light-harvesting chlorophyll *a/b* protein complex from chloroplast membranes. *Biochim. Biophys. Acta.* 1098:159–166.

Ide, J. P., D. R. Klug, W. Kühlbrandt, J. B. Giorgi, and G. Porter. 1987. The state of detergent solubilised light-harvesting chlorophyll-*a/b* protein complex as monitored by picosecond time-resolved fluorescence and circular dichroism. *Biochim. Biophys. Acta.* 893:349–364.

Jennings, R. C., R. Bassi, F. M. Garlaschi, P. Dainese, and G. Zucchelli. 1993. A study of Photosystem II fluorescence emission in terms of the antenna chlorophyll-protein complexes. *Biochemistry.* 32:3203–3210.

Kühlbrandt, W., and D. N. Wang. 1991. Three-dimensional structure of plant light-harvesting complex determined by electron crystallography. *Nature.* 350:130–134.

Kühlbrandt, W., D. N. Wang, and Y. Fujiyoshi. 1994. Atomic model of plant light-harvesting complex. *Nature.* 367:614–621.

Kwa, S. L. S., F. G. Groeneveld, J. P. Dekker, R. van Grondelle, H. van Amerongen, S. Lin, and W. S. Struve. 1992a. Ultrafast energy transfer in LHC-II trimers from the Chl *a/b* light-harvesting antenna of photosystem II. *Biochim. Biophys. Acta.* 1101:143–146.

Kwa, S. L. S., H. van Amerongen, S. Lin, J. P. Dekker, R. van Grondelle, and W. S. Struve. 1992b. Steady-state and time-resolved polarized light spectroscopy of the green plant light harvesting complex II. *Biochim. Biophys. Acta.* 1102:202–212.

Kwa, S. L. S., S. Völker, N. T. Tilly, R. van Grondelle, and J. P. Dekker. 1994. Polarized site-selection spectroscopy of chlorophyll a in detergent. *Photochem. Photobiol.* 59:219–228.

Paulsen, H., B. Finkenzeller, and N. Kühlein. 1993. Pigments induce folding of light-harvesting chlorophyll *a/b*-binding protein. *Eur. J. Biochem.* 215: 809–816.

Reddy, N. R. S., H. van Amerongen, S. L. S. Kwa, R. van Grondelle, and G. J. Small. 1994. Low energy exciton level structure and dynamics in LHC-II trimers from the Chl *a/b* antenna complex of Photosystem II. *J. Phys. Chem.* 98:4729–4735.

Renge, I. 1992. On the determination of molecular polarizability changes upon electronic excitation from the solvent shifts of absorption band maxima. *Chem. Phys.* 167:173–183.

Savikhin, S., H. van Amerongen, S. L. S. Kwa, R. van Grondelle, and W. S. Struve. 1994. Low-temperature energy transfer in LHC-II trimers from the Chl *a/b* light-harvesting antenna of Photosystem II. *Biophys. J.* 66:1597–1603.

Van Amerongen, H., B. van Haeringen, M. van Gurp, and R. van Grondelle. 1991. Polarized fluorescence measurements on ordered photosynthetic antenna complexes. Chlorosomes of *Chloroflexus aurantiacus* and B800–850 antenna complexes of *Rhodobacter sphaeroides*. *Biophys. J.* 59: 992–1001.

Van Gurp, M., G. van Ginkel, and Y. K. Levine. 1988. Orientational properties of biological pigments in ordered systems studied with polarized light: photosynthetic pigment-protein complexes in membranes. *J. Theor. Biol.* 131:333–349.

Van Gurp, M., G. van Ginkel, and Y. K. Levine. 1989. Fluorescence anisotropy of chlorophyll *a* and chlorophyll *b* in castor oil. *Biochim. Biophys. Acta.* 973:405–413.

Zucchelli, G., R. C. Jennings, and F. M. Garlaschi. 1990. The presence of long-wavelength chlorophyll *a* spectral forms in the light-harvesting chlorophyll *a/b* protein complex II. *J. Photochem. Photobiol. B Biol.* 6: 381–394.